Integration of seismic, CSEM and well data in the Perdido basin, Gulf of Mexico

Philippe Nivlet, Luis Sánchez Pérez, EMGS Services México, José Antonio Escalera Alcocer, José Trinidad Martínez Vázquez, Arturo Escamilla Herrera, Marco Vázquez García, Humberto Salazar Soto, Pemex subdirección Exploración

Summary

We present the results of a joint interpretation of both 3D seismic and 3D CSEM data from a prospect in the Perdido fold belt (deep offshore Gulf of Mexico). The study began after the first exploration well was drilled over the structure, confirming the presence of oil in two Early Eocene intervals. The integrated methodology tailored for the study has resulted in (1) a better understanding of the sensitivity of the CSEM data, (2) discrimination between lithology and fluid effects and finally (3) an update of the oil volume estimated over the structure.

Introduction

The marine controlled source electromagnetic (CSEM) method for hydrocarbon exploration was used for the first time in 2000 (Ellingsrud et al., 2002) and is now an established exploration tool, used as a complement to seismic data. For example, in the Gulf of Mexico, in 2010 Pemex opted to use it as an independent source of information, complementing seismic in order to mitigate exploration risk and improve management of its deep-offshore exploration portfolio (Escalera Alcocer et al., 2013).

During the last few years, numerous methodologies have been presented to interpret CSEM data either qualitatively or quantitatively, and the most recent trend in that respect is the development of methods to integrate CSEM and seismic data in a common interpretation: qualitative interpretation (Escalera Alcocer et al., 2013); quantitative interpretation of CSEM and seismic based on rock physics relationship (Harris et al., 2009; Morten et al., 2011; Tomlinson et al., 2013); or full petrophysical joint CSEM-seismic inversion (Miotti et al., 2013). The success of such joint approaches is based on the complementarity of these data: whereas seismic data are, in the best case, only sensitive in a qualitative way to the fluid content, CSEM is very sensitive to fluid saturation. On the other hand, seismic amplitudes can provide quite a detailed understanding of the spatial distributions of lithology and porosity, from which interpretation of CSEM can benefit. However, integrating CSEM and seismic data is not always an easy task due to the following issues:
- Data are affected by uncertainties;
- Data have very different vertical resolution (from 10 m for seismic to several hundreds of meters for CSEM);

- Interpretation of anomalies is never unique: for instance a resistive anomaly detected from CSEM inversion may be caused by hydrocarbon accumulation but also by a reduced porosity;
- The physical models used to invert data are approximations and rely on assumptions that cannot be always verified, especially in the exploration context due to scarcity of well data.

In the present paper, we present an alternative integration methodology, which has been developed to cope with the interpretation challenges linked with the depth of the prospect (5200-5700 m TVDSS; 2300-2800 m below mudline). Based on a combination of rock physics, CSEM modelling and synthetic inversion, we progressively try to understand the resistivity anomalies observed in CSEM inversion, ending with an estimation of reserves in place, together with its uncertainty.

Background information

We focus in this paper on a prospect located in the Perdido fold belt of the Mexican part of the Gulf of Mexico. The water depth over the prospect is around 3000 m. The main targets are two levels W1 and W2 in the Wilcox formation (Early Eocene) located respectively 2300 and 2800 m below mudline, with potential reservoirs formed of turbiditic sandstones from a complex of submarine fans derived from Tertiary deltaic systems. The perforation of an exploration well proved the presence of light oil in the
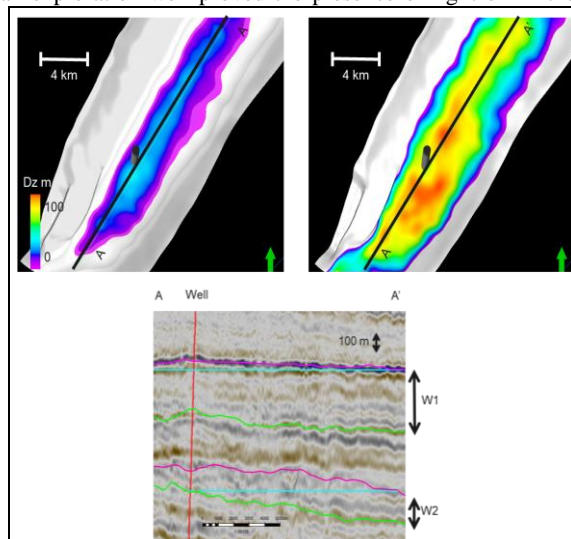

Figure 1: Top W1 (upper left) and W2 (upper right) structural maps with and arbitrary section through seismic data (lower)

Integration of seismic, CSEM and well data in the Perdido basin, Gulf of Mexico

two targets. Figure 1 displays maps of thickness from proven contacts to the top reservoir: W1 has a thin oil column of 30 m, whereas W2 has a maximal oil column of 110 m.

Data available for this study include the following:
- The well logs from the perforated well, including horizontal and vertical resistivity as well as petrophysical interpretation logs like effective porosity Φ_e, clay fraction V_{Cl}, or water saturation S_w;
- Φ_e and V_{Cl} cubes (in depth), obtained from petrophysical inversion of 3D seismic data over the area;
- Vertical and horizontal resistivity cubes from 3D CSEM inversion revised after the perforation of the well.

A resistive anomaly is detected in the center of Figure 2: It is confined to the Eastern part of the prospect, and tends to attenuate towards the Northwest. The well is located just at the edge of the anomaly. The question we will address in this paper is to try to understand whether this anomaly can be correlated quantitatively to hydrocarbon accumulation? If yes, would it be related to W1? To W2? Or to a combination of the two?
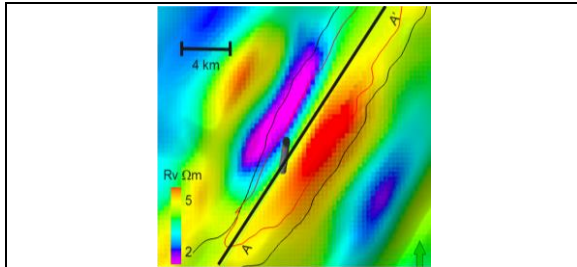

Figure 2: Average Rv (Eocene window) from CSEM inversion results; red and black contours are the contacts for W1 and W2 intervals

Both the CSEM and the seismic inversion are considered to be of good quality based on comparison of inversion results at well position to measured well data.

Rock physics model calibration

From well data, the first step is to calibrate a modified Simandoux model linking horizontal resistivity R_h to Φ_e, V_{Cl} and S_w.

$$\frac{1}{R_h} = a.S_w^2\Phi_e^2(\alpha Z + 24.5) + bV_{cl}S_w \qquad (1)$$

In this equation, dependency to water resistivity is accounted for by the dependency to depth Z (α being the

temperature gradient), whereas a and b are constants calibrated by linear regression.

The vertical resistivity R_v is obtained by multiplying this result by an anisotropy factor depending linearly on V_{Cl}, c and d being estimated by linear regression:

$$R_v = (cV_{cl} + d)R_h \qquad (2)$$

Figure 3 illustrates the good fit obtained between measured and predicted resistivity (correlation coefficients between prediction and model over 0.95).
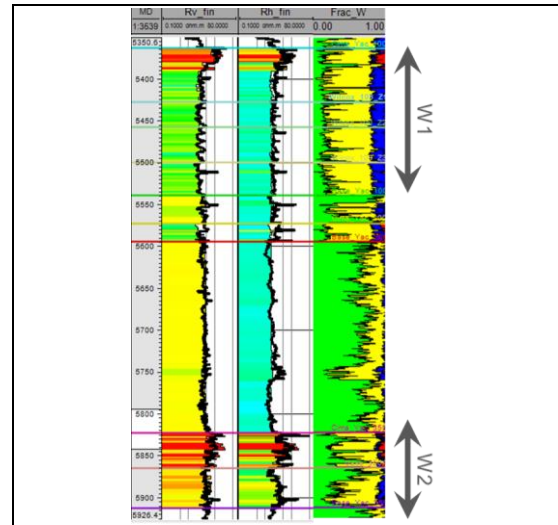

Figure 3: Modeled (color) compared to measured (bold black) vertical (left) and horizontal (center) resistivity. The track on the right displays volumetric fractions of clay (green), sand (yellow), brine filled effective porosity (blue) and oil filled porosity (red)

Resistivity model building

The quality of fit of the aforementioned model remained almost identical after upscaling well logs to the seismic scale, and the calibrated model was then judged to be accurate enough to predict resistivity from the seismically derived Φ_e and V_{Cl} cubes.

Two reservoir models have been built corresponding to two possible scenario addressing fluids in the reservoirs:
- Model 1 (Figure 4): Reservoirs are filled with light oil (S_w=0.2) to the contact depth indicated in Table 1; S_w =1 below this level;
- Model 2: S_w=1 everywhere.

Integration of seismic, CSEM and well data in the Perdido basin, Gulf of Mexico

These resistivity models are then inserted in the same 3D background as the one used previously for the CSEM inversion.
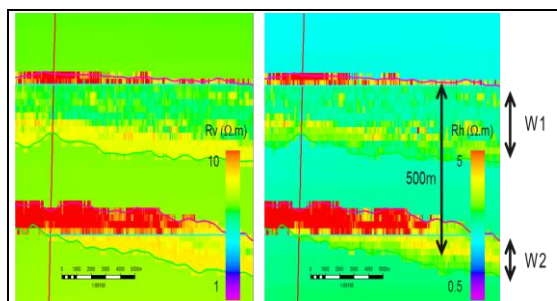

Figure 4: Vertical (left) and horizontal (right) resistivity model for the oil saturated case – model 1 (section)

Synthetic inversion

Synthetic inversion includes a 3D CSEM modelling step based on the real acquisition configuration followed by a 3D CSEM inversion. It provides a realistic estimate of how much of the modeled resistivity anomaly can be retrieved from the inversion.
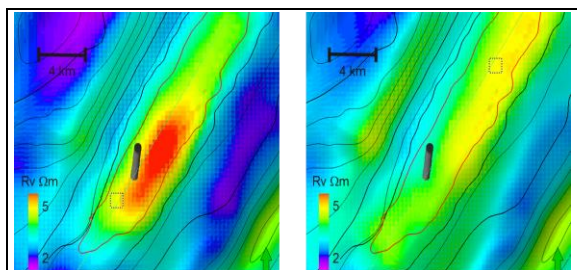

Figure 5: Average vertical restivity (Eocene window) from Model 1 (left) and Model 2 (right)

Figure 5 shows that the inverted resistive anomaly of Model 1 is very consistent with the inversion from the survey (Figure 2). In the Model 2, synthetic inversion result show that the anomaly is not present. Hence it is very likely that hydrocarbons are present in sufficient quantities to be detected from CSEM. Resistivity drops northwards, where the hydrocarbon column becomes too thin to be detected, both in the real inversion case and in the synthetic data (figure 5, Model 1).

Sensitivity study

The methodology presented in Mittet and Morten (2012) consists of modelling the CSEM response of a 3D target in a 1D background. The sensitivity of CSEM response is given by equation (3):

$$S = \frac{\left| E_{tgt} - E_{bg} \right|}{\varepsilon} \tag{3}$$

Where (E_{tgt} - E_{bg}) is the maximal difference between CSEM responses for all recorded offsets and frequencies with and without target and ε is the data uncertainty. Sensitivity less than 1 is considered as low (not detectable target), whereas a value over 3 corresponds to a very sensitive target.

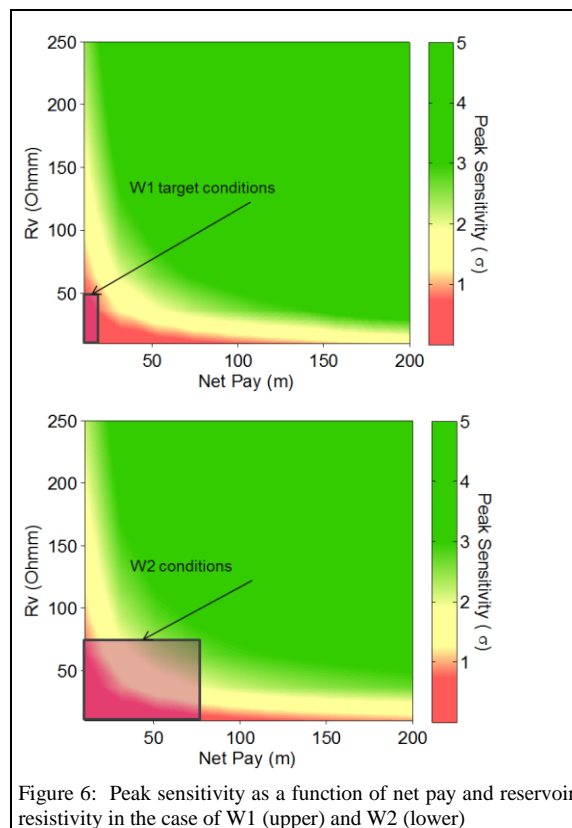| Prospect	W1	W2
Contact depth (m)	5257	5700
Reservoir resistivity (Ωm)	5-50	10-70
Net pay thickness (m)	3-10	10-80
Background resistivity (Ωm)	4-4.2	
Geometrical correction factor	0.8-1.7	

Table 1: Parameters describing targets W1 and W2

Figure 6: Peak sensitivity as a function of net pay and reservoir resistivity in the case of W1 (upper) and W2 (lower)

Integration of seismic, CSEM and well data in the Perdido basin, Gulf of Mexico

Table 1 summarizes the net pay and resistivity derived from seismic for the two targets used for the sensitivity study. Figure 6 shows that the shallower target W1 has low sensitivity and probably, does not add to the CSEM response. This is due to the low net pay of the target (Table 1). Target W2, on the contrary, is detectable with a moderate sensitivity.

Volumetric

Volumetric evaluation is an integral part of the exploration process. Baltar and Roth (2013) presented a methodology to evaluate reserve volume probability from CSEM inversion results: The methodology distinguishes two cases (positive and negative), depending on whether the resistor corresponding to the hydrocarbon accumulation has a sufficient area, thickness, and resistivity contrast to the background environment to be detected from CSEM. The method is based on two main concepts or observations:

- CSEM resistivity has a much better lateral resolution than it has vertically;
- Given a 1D resistivity trace extracted from a 3D CSEM inversion, the anomalous transverse resistivity (ATR) equivalence principle (Constable, 2010) can be written as Equation 4 (below), providing a way to estimate the net pay column at this position:

$$\int_{CSEManomaly} \left(R_{CSEM}(z) - R_{bg}(z) \right) dz = \int_{payzone} \left(R_{reservoir}(z) - R_{bg}(z) \right) dz \tag{4}$$

In Equation 4, R_{bg} is the vertical background resistivity from CSEM inversion, $R_{reservoir}$ the vertical resistivity in the reservoir and R_{CSEM}, the vertical resistivity estimated by the CSEM inversion. The integration window for the left term is identical to the one used for the average resistivity maps displayed above. The rest of the resistivity parameters are generated from pre-defined distributions using Monte-Carlo simulation (Table 1).
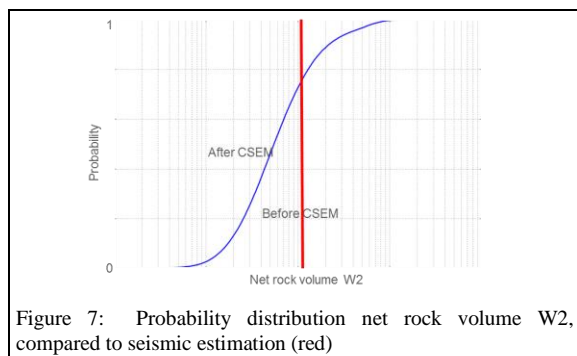

Figure 7: Probability distribution net rock volume W2, compared to seismic estimation (red)

In the case study, since only W2 has a significant impact on CSEM response, only this anomaly has been considered in the reserve estimation. Prior to using eq. (4) to estimate net pay thickness, it is necessary to recalibrate the ATR estimated from CSEM inversion to account for the loss of information occurred in the inversion process and which has been put in evidence by the synthetic inversion. This exercise allows estimating a geometrical correction factor distribution (see table 1). Globally, Figure 7 shows that the average seismic volume estimate corresponds to the P70 case estimated from CSEM data, which is a reasonable agreement. Hence, in this study, CSEM data allows making the seismic volume estimation more robust by confirming it with independent data.

Conclusions

We have described a workflow for integrating CSEM and seismic data and applied it to a real case study. We have shown that combining the knowledge derived from well, seismic and CSEM could beneficiate greatly in understanding anomalies from CSEM and therefore using this data in a more effective way.

Synthetic data inversions based on a rock physics modeling and comparison to real data inversion show good likelihood of high hydrocarbon saturation in the reservoir mapped by seismic. Based on sensitivity assessments for expected reservoir parameter ranges, we conclude that the observed resistivity anomaly can mainly be attributed to the deeper Eocene interval, whereas the CSEM sensitivity to the shallower interval is limited. Performing an independent net rock volume estimation based on CSEM anomaly gives a distribution, which is consistent with previous seismic estimations.

Acknowledgements

http://dx.doi.org/10.1190/segam2014-1497.1

EDITED REFERENCES
Note: This reference list is a copy-edited version of the reference list submitted by the author. Reference lists for the 2014 SEG Technical Program Expanded Abstracts have been copy edited so that references provided with the online metadata for each paper will achieve a high degree of linking to cited sources that appear on the Web.

REFERENCES

Baltar, D., and F. Roth, 2013, Reserves estimation methods for prospect evaluation with 3D CSEM data: First Break, **31**, no. 6, 103–111.

Ellingsrud, S., T. Eidesmo, S. Johansen, M. C. Sinha, L. M. MacGregor, and S. Constable, 2002, Remote sensing of hydrocarbon layers by seabed logging (SBL): Results from a cruise offshore Angola: The Leading Edge, **21**, 972–982, http://dx.doi.org/10.1190/1.1518433.

Escalera Alcocer, J. A., M. Vázquez García, H. Salazar Soto, D. Baltar, V. Ricoy Paramo, P. T. Gabrielsen, and F. Roth, 2013, Reducing uncertainty by integrating 3D CSEM in the Mexican deep-water exploration workflow: First Break, **31**, no. 4, 75–79.

Constable, S., 2010, Ten years of marine CSEM for hydrocarbon exploration: Geophysics, **75**, no. 5, 75A67–75A81, http://dx.doi.org/10.1190/1.3483451.

Harris, P., Z. Du, L. MacGregor, W. Olsen, R. Shu, and R. Cooper, 2009, Joint interpretation of seismic and CSEM data using well log constraints: An example from the Luva Field: First Break, **27**, no. 5, 73–81.

Miotti, F., I. Guerra, F. Ceci, A. Lovatini, M. Paydayesh, M. Leathard, and A. Sharma, 2013, Petrophysical joint jnversion of seismic and EM attributes: A case study: Presented at the 83rd Annual International Meeting, SEG.

Mittet, R., and J. P. Morten, 2012, Detection and imaging sensitivity of the marine CSEM method: Geophysics, **77**, no. 6, E411–E425, http://dx.doi.org/10.1190/geo2012-0016.1.

Morten, J. P., F. Roth, D. Timko, C. Pacurar, A. K. Nguyen, and P. A. Olsen, 2011, 3D reservoir characterization of a North Sea oil field using quantitative seismic & CSEM interpretation: 81st Annual International Meeting, SEG, Expanded Abstracts, 1903–1907.

Tomlinson, J., L. MacGregor, and P. Newton, 2013, Reservoir characterization using the integrated analysis of CSEM, seismic and well log data: 13th International Congress of the SBGf, Extended Abstracts, 102–105.